

DADP: Domain Adaptive Diffusion Policy

Pengcheng Wang^{1*} Qinghang Liu^{1,2*} Haotian Lin³
 Yiheng Li¹ Guojian Zhan^{1,4} Masayoshi Tomizuka¹ Yixiao Wang¹

Abstract

Learning domain adaptive policies that can generalize to unseen transition dynamics, remains a fundamental challenge in learning-based control. Substantial progress has been made through domain representation learning to capture domain-specific information, thus enabling domain-aware decision making. We analyze the process of learning domain representations through dynamical prediction and find that selecting contexts adjacent to the current step causes the learned representations to entangle static domain information with varying dynamical properties. Such mixture can confuse the conditioned policy, thereby constraining zero-shot adaptation. To tackle the challenge, we propose **DADP (Domain-Adaptive Diffusion Policy)**, which achieves robust adaptation through unsupervised disentanglement and domain-aware diffusion injection. First, we introduce Lagged Context Dynamical Prediction, a strategy that conditions future state estimation on a historical offset context; by increasing this temporal gap, we unsupervisedly disentangle static domain representations by filtering out transient properties. Second, we integrate the learned domain representations directly into the generative process by biasing the prior distribution and reformulating the diffusion target. Extensive experiments on challenging benchmarks across locomotion and manipulation demonstrate the superior performance, and the generalizability of DADP over prior methods. More visualization results are available on the [website](#).

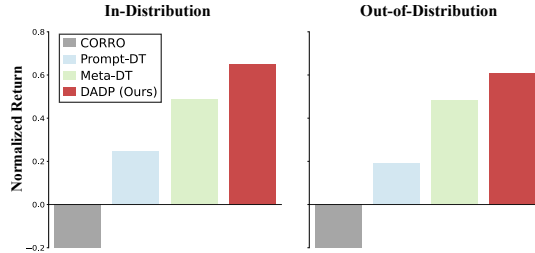


Figure 1. Averaged Normalized Performance of baselines across In-Distribution and Out-of-Distribution settings across all tasks. The results are normalized with random and expert policy performance.

1. Introduction

Learning-based policies have achieved remarkable success recently, enabling agents to solve increasingly complex decision-making problems (Liu et al., 2025b; Su et al., 2025). Despite these advances, most existing approaches remain coupled to a specific environment or operating condition (Wang et al., 2024a; Barreto et al., 2017), and their performance often degrades when deployed in the unseen domains (He et al., 2025), which limits the practical applicability of learning-based policies. This mismatch highlights a fundamental challenge: designing a single policy that can generalize efficiently and robustly across domains remains critically important but inherently difficult.

Most prior approaches begin by extracting domain information and leveraging it for decision-making, namely domain representation learning and representation utilization. Regarding the former, many methods extract representations through contrastive learning (Yuan & Lu, 2022; Wen et al., 2024), whose performance often depends on carefully designed objectives and extra data generation. Some other approaches instead employ dynamical prediction as an auxiliary task to implicitly learn the domain representations from transitional dynamics (Lee et al., 2020; Evans et al., 2022); however, the resulting representations are frequently of limited quality due to entangling the static domain information with varying dynamical properties. Regarding the latter, most methods utilize representations through input concatenation (Kumar et al., 2021; 2022), namely using representations as extra network input, or rely on sequence-modeling architectures (Wang et al., 2024b; Ota, 2024; Huang et al., 2024) to capture domain information in an implicit, end-to-

* equal contribution, order is decided randomly ¹University of California, Berkeley, California, USA ²Peking University, Beijing, China ³CMU, Pennsylvania, USA ⁴Tsinghua University, Beijing, China. Correspondence to: Yixiao Wang <yixiao_wang@berkeley.edu>.

end manner. Such approaches often fail to fully leverage the learned representations, resulting in degraded performance.

To tackle these challenges, we propose **DADP** (**D**omain-**A**daptive **D**iffusion **P**olicy), which achieves robust adaptation through unsupervised disentanglement and domain-aware diffusion injection. First, to remove disentangle time-varying properties from the unsupervisedly learned representation, we introduce Lagged Context Dynamical Prediction. Specifically, we break the temporal correlation between the context and the current step by introducing a large historical offset $\Delta t \rightarrow \infty$, preventing time-varying information in the context from assisting dynamical prediction and thereby excluding it from the extracted representation during learning. Second, we inject the learned representations directly into the generative process. Specifically, we start denoising with a representation-biased mixed Gaussian distribution, and reformulate the diffusion target to include the learned representation. We evaluate DADP across locomotion and manipulation tasks across MuJoCo and Adroit, showing consistently superior performance in both modalities capturing ability and generalizability.

In summary, our main contributions are as follows:

- **Unsupervised Representation Learning.** We propose Lagged Context Dynamical Prediction, a simple yet effective approach for unsupervisedly learning domain representations from dynamical prediction.
- **Denoising with Representation-Prediction.** Instead of conditioning, we utilize the domain representations by biasing the prior distribution and reformulating the diffusion target, enabling better policy performance.
- **Superior Performance.** We evaluate DADP on a broader and more challenging set of domain adaption tasks, demonstrating consistently superior performance in domain-adaptivity under the zero-shot setting.
- **Open-sourced Dataset and Pipeline.** We release a complete open-sourced codebase, including the algorithm, datasets, and data generation pipeline, allowing the community to easily customize our framework.

2. Related Work

2.1. Domain Adaptive Policy

Sequential Modeling Policy. Regarding policy architecture, early efforts extend the observation to context composed of multiple consecutive state (Kumar et al., 2021) to provide sufficient information for domain adaption. Subsequent works leverage mature sequence-to-sequence models to better utilize the contextual information, such as Transformers (Chen et al., 2021; Wang et al., 2024b) or Mamba (Ota, 2024; Huang et al., 2024). Among them, Locoformer (Liu et al., 2025b) employs Transformer-XL (Dai et al., 2019)

to enable information sharing across episodes and online improvement. However, these methods often rely on purely end-to-end learning, where the absence of intermediate supervision prevents the models from effectively exploiting the implicit dynamical information (Dai et al., 2019).

Meta RL and In-Context RL. Regarding algorithms, In Context Reinforcement Learning (ICRL) (Laskin et al., 2022) and Meta Reinforcement Learning (Duan et al., 2016) methods constitute a widely adopted approach, designed to operate over a MDP set by learning from task-level variations during training. In-context Q Learning (Liu et al., 2025a) feed the task representation into a causal transformer with value and policy head for efficient learning across domains. This reflects the dominant approach adopted by most prior works (Kumar et al., 2021; Yuan & Lu, 2022) on ICRL, where the learned representations are provided as additional input to the network to enable domain-aware decision making. Closest to our work, MetaDiffuser (Ni et al., 2023) also incorporates learned domain representations into the diffusion process. However, its representations suffer from the entangled time-varying information due to its representation learning pipeline, which can be solved with our proposed Lagged Context Dynamical Prediction.

2.2. Domain Representation Learning.

Domain refers to the environment’s transition dynamics. In practice, it is often characterized by a low-dimensional parameter vector, including environmental parameters (e.g., gravity, friction) or agent-specific parameters (e.g., joint torques, limb lengths). To address the problem of domain adaptive policy learning, many prior works focused on domain representation learning, where a compact representation of domain is inferred from a trajectory of interactions.

Supervised. Some works adopt a supervised learning setting, assuming that each domain can be characterized by a low-dimentional accessible environmental factor (Zhang et al., 2025; Lyu et al., 2025), which naturally serves as the target for representation learning. One of the most well-known works is RMA (Kumar et al., 2021; 2022), which achieves online adaptation to different environments by co-training a factor-supervised context encoder and an representation-conditioned policy.

Unsupervised. Many other prior works focus on the unsupervised setting, where such environmental factors are assumed to be unavailable. One line of work leverages classical unsupervised learning techniques to cluster data of different domains, such as contrastive learning-based approaches (Li et al., 2020; Wang et al., 2023). Among them, CORRO (Yuan & Lu, 2022) proposes a contrastive learning framework for robust task representations under distribution shifts between training and test behavior policies. However, such methods often rely on, yet fail to fully

exploit, the temporal and sequential structure inherent in control tasks, and are highly dependent on the quality of the extra data generation model. In contrast, our approach is derived from dynamics prediction formulated through sequence modeling, enabling a simpler and more effective capture of domain information.

Another line of work learn domain representations implicitly by introducing dynamics prediction as an auxiliary task, like CaDM (Lee et al., 2020), IIDA (Evans et al., 2022) and CARoL(Hu et al., 2025). However, such methods often suffer from poor representation quality, as they also fail to properly remove the varying information present in the context. In contrast, our method breaks such time-local cues by reconstructing prediction pairs, thereby yielding representations that serve as domain-specific static representations.

3. Preliminaries

3.1. Problem Formulation

In this work, we formulate the domain adaptive policy learning as an offline meta-RL problem. Specifically, we consider a task set $\mathcal{T} = \{\mathcal{T}_i\}_{i=1}^n$, where each task \mathcal{T}_i consists of an Markov Decision Process (MDP) and a policy that has been pre-trained on this MDP.

$$\mathcal{T} = \{\mathcal{T}_i\}_{i=1}^n = \{(\mathcal{M}_i, \pi_i)\}_{i=1}^n \quad (1)$$

The MDP can be defined by a tuple $\mathcal{M}_i = (\mathcal{S}, \mathcal{A}, R, p_i)$, where $\mathcal{S} \subseteq \mathcal{R}^n$ is a continuous state space, $\mathcal{U} \subseteq \mathcal{R}^m$ is a continuous action space, $R : \mathcal{S} \times \mathcal{U} \rightarrow \mathbb{R}$ is the reward function, and $p_i : \mathcal{S} \times \mathcal{U} \times \mathcal{S} \rightarrow [0, \infty)$ is the transition probability function. Across all MDPs, the state space \mathcal{S} , action space \mathcal{A} , and reward function R are shared, while the transition dynamics p_i differ across tasks, i.e., $p_i \neq p_j$.

For each task \mathcal{T}_i , the agent is given an offline dataset \mathcal{D}_i , collected by executing a *domain-specific* expert policy π_i in the corresponding environment \mathcal{M}_i . The expert policy π_i is constructed by training a reinforcement learning (RL) agent to (near-)optimality on \mathcal{T}_i , and is therefore specialized to the dynamics and reward of \mathcal{M}_i . Our objective is to learn a policy π using the datasets $\{\mathcal{D}_i\}$ from the training task set $\mathcal{T}^{\text{train}}$, and to maximize discounted return for all tasks in $\mathcal{T}^{\text{train}} \cup \mathcal{T}^{\text{test}}$, i.e., $J(\pi) = \mathbb{E}_\pi[\sum_{t=0}^{\infty} \gamma^t R(s_t, a_t, s_{t+1})]$, where $\gamma \in (0, 1)$ is the discount factor.

3.2. Diffusion Policy

Diffusion policies (Chi et al., 2025; Ho et al., 2020) model the action generation as a stochastic denoising process conditioned on the observation. Specifically, a diffusion policy learns a conditional action distribution $q(a|s)$ through a predefined forward diffusion process and a learned reverse denoising process. The forward process gradually perturbs

a clean action a^0 into noisy latent variables a^t by

$$q(a^t | a^{t-1}) = \mathcal{N}(a^t | \sqrt{\bar{\alpha}_t} a^{t-1}, \Sigma_t), \quad (2)$$

where $\mathcal{N}(\mu, \Sigma)$ denotes a Gaussian distribution with mean μ and variance Σ_t , $\bar{\alpha}_t \in \mathbb{R}$ is the variance schedule, and $a^0 \sim q(a|s)$ is an action sampled from the data distribution.

Starting from Gaussian noise, actions are generated by iteratively applying the learned reverse process. The denoising policy $\epsilon_\theta(a_t, s, t)$ predicts the noise at each diffusion step conditioned on input. The policy is trained by minimizing a simplified surrogate objective (Ho et al., 2020):

$$\mathcal{L}_{\text{diff}}(\theta) = \mathbb{E}_{a^0, \epsilon, k} [\|\epsilon - \epsilon_\theta(a^k, s, k)\|^2], \quad (3)$$

where $a^t = \sqrt{\bar{\alpha}_t} a^0 + \sqrt{1 - \bar{\alpha}_t} \epsilon$, $\epsilon \sim \mathcal{N}(0, I)$. The objective encourages the model to recover the injected noise at each diffusion step. At inference time, the policy samples an action by initializing from Gaussian noise and iteratively applying the learned denoising model conditioned on the current state to get the clean action distribution.

4. Domain Adaptive Diffusion Policy

4.1. Learn Representation by Extracting Static Info

To enable the policy to possess domain adaptive capability, we firstly train a context encoder $E_\phi(\cdot)$ to learn an effective domain representation z_t from the context τ_t . We choose to learn the representation from context since (i) the domain factors that govern dynamics are typically latent and must be inferred from observed transitions, and (ii) at test time, the agent generally has access only to interaction history rather than privileged environment parameters.

In this work, we learn the representation implicitly from dynamical prediction. Typically, the context as encoder input is from the most recent history (Ni et al., 2023):

$$\begin{aligned} z_t &= E_\phi(\tau_t); \hat{s}_{t+1} = f_\theta(s_t, a_t, z_t); \\ \tau_t &= (s_{t-H}, a_{t-H}, \dots, s_{t-1}, a_{t-1}). \end{aligned} \quad (4)$$

This context selection is intuitive, as it aligns with the usage in online policy inference, where the most recent history is used as context. Note that there are two types of necessary information that can be inferred from the context, which are both necessary for accurate next state prediction: **static information** ξ that represents the domain-specific dynamics (e.g. gravity), **varying information** ω_t that includes instantaneous dynamical properties not captured in the current state (e.g. higher-order temporal derivatives of states):

$$s_{t+1} = f(s_t, a_t, \xi, \omega_t); z_t = E_\phi(\tau_t) = (\xi^z, \omega_t^z), \quad (5)$$

where f represents the ground-truth forward dynamics, ξ^z and ω_t^z represent the inferred information from the context.

Note that since the context is drawn from the most recent history, the inferred varying information ω_t^z is temporally aligned with the ground-truth varying information ω_t required for prediction task:

$$z_t = \arg \min_{z=(\omega_t^z, \xi^z)} \mathbb{E}_{\mathcal{D}} \|s_{t+1} - s_{t+1}^z\|^2. \quad (6)$$

As a result, $z_t = (\xi, \omega_t)$ becomes a natural global minimum for the dynamical prediction task.

However, recall that a domain corresponds to the environment's transition dynamics, usually parameterized by a low-dimensional vector and therefore inherently static. For domain adaptation, the primary purpose of the representation is to provide a stable descriptor of the domain: it should reflect the persistent domain factors ξ across time, while remaining insensitive to ephemeral variations ω_t that are not stable within a domain. Encoding ω_t into z_t can cause *representation drift* within the same domain, reducing separability across domains and harming generalization when z_t is used as a domain descriptor for downstream policy learning. This motivates us to seek a mechanism for disentangling time-varying information ω_t from z_t .

To remove ω_t , we propose Lagged Context Dynamical Prediction. Specifically, we introduce a temporal offset Δt to weaken the contribution of time-local cues in the context for next state prediction. With Δt , we can adjust the "distance" between the context and the current timestep:

$$\begin{aligned} z_{t-\Delta t} &= E_{\phi}(\tau); \hat{s}_{t+1} = f_{\theta}(s_t, a_t, z_{t-\Delta t}); \\ \tau_{t-\Delta t} &= (s_{t-H+1-\Delta t}, a_{t-H+1-\Delta t}, \dots, s_{t-\Delta t}, a_{t-\Delta t}), \end{aligned} \quad (7)$$

, where the original context corresponds to $\Delta t = 1$.

From an information-theoretic viewpoint, as Δt increases, the offset context becomes less informative about instantaneous variations. Since $z_{t-\Delta t}$ is a function of $\tau_{t-\Delta t}$, we have $I(\omega_t; z_{t-\Delta t} | s_t, a_t, \xi) \leq I(\omega_t; \tau_{t-\Delta t} | s_t, a_t, \xi)$. In this way, $z_{t-\Delta t}$ discards the instantaneous variations, while ξ remains informative since it is time-invariant within a domain. Consequently, optimizing prediction with offset contexts biases the representation toward the static domain factors ξ rather than transient ω_t .

When $\Delta t \rightarrow \infty$, the representation $z_{-\infty} = (\xi, \bar{\omega})$ becomes static, where ξ is the static domain information, $\bar{\omega}$ is a averaged varying properties that minimizes the prediction loss on the dataset distribution. This can be easily achieved by selecting the context from another episode in the same domain. Please refer to Appendix A for a toyexample explanation.

4.2. Utilize Representation by Diffusion Modulation

After obtaining high-quality domain representations, it remains to determine how to better utilize them to enable

domain-aware decision-making. In this work, we build our method upon diffusion policy, as it has been widely adopted and has demonstrated strong performance across various control tasks.

In the standard Diffusion Policy (Chi et al., 2025), the denoising process starts from pure Gaussian noise, where different denoising trajectories are governed by single representation-conditioned policy:

$$a^t = \sqrt{\bar{\alpha}_t} a^0 + \sqrt{1 - \bar{\alpha}_t} \epsilon. \quad (8)$$

If we simply take the learned representation as extra policy inputs, the diffusion policy has to reconstruct different domain-specific action modalities from every sampled point in the prior gaussian distribution equally. This entanglement leads to mixed denoising trajectories in the latent noise space, preventing the policy from exploiting the structure of the noise to better leverage domain information, and consequently resulting in degraded performance.

To solve this challenge, instead of utilizing the representation as condition, we inject the representation to the generation. Specifically, DADP initializes the denoising process from a Gaussian Mixture by incorporating the learned representation z into the forward process. Following the formulation for structured diffusion models (e.g. Mixed DDIM (Jia et al., 2024)), we define the perturbed state x_t as:

$$a^t = \sqrt{\bar{\alpha}_t} (a^0 - z) + z + \sqrt{1 - \bar{\alpha}_t} \epsilon, \quad (9)$$

where the fully noised data point at step T follows $x_T = z + \epsilon$, and the prior distribution is a mixed Gaussian distribution with multiple peaks, where each peak represents a domain-specific action modality. In this way, we inject the domain information into prior distribution as shown in Figure 2.

By rearranging Eq. (9), the clean action a^0 can be estimated from a^t and the predicted noise ϵ^0 :

$$a^0 = \frac{a^t - z - \sqrt{1 - \bar{\alpha}_t} \epsilon^0}{\sqrt{\bar{\alpha}_t}} + z. \quad (10)$$

Utilizing the Denoising Diffusion Implicit Model (DDIM) formulation (Song et al., 2022) and omitting the stochastic noise injection for clarity, the reverse step is defined as:

$$a^{t-1} = \sqrt{\bar{\alpha}_{t-1}} a^0 + \sqrt{1 - \bar{\alpha}_{t-1}} \frac{a^t - \sqrt{\bar{\alpha}_t} a^0}{\sqrt{1 - \bar{\alpha}_t}}. \quad (11)$$

Substituting Eq. (10) into Eq. (11) yields:

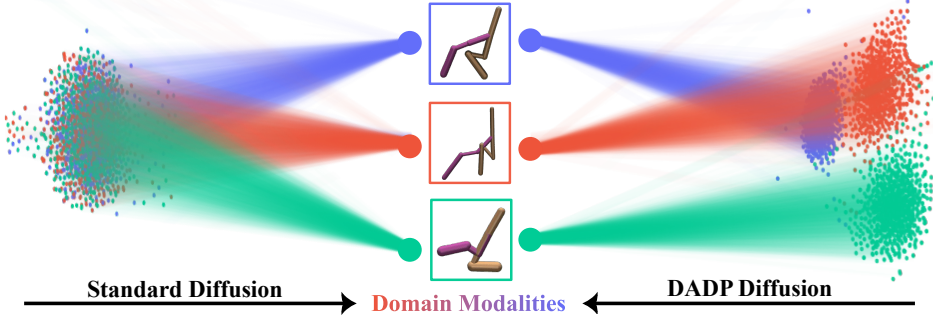


Figure 2. t-SNE Visualization of Denoising Process of Standard Diffusion and DADP. The sampled points from prior distribution and utilized representation are contructed from the training datasets and learned context encoder.

$$a^{t-1} = \sqrt{\frac{\bar{\alpha}_{t-1}}{\bar{\alpha}_t}} (a^t - z - \sqrt{1 - \bar{\alpha}_t} \epsilon^\theta) + \sqrt{\bar{\alpha}_{t-1}} z + \frac{\sqrt{1 - \bar{\alpha}_{t-1}}}{\sqrt{1 - \bar{\alpha}_t}} (z + \sqrt{1 - \bar{\alpha}_t} \epsilon^\theta - \sqrt{\bar{\alpha}_t} z). \quad (12)$$

In this work, instead of setting ϵ^θ as the prediction target as usual, we propose a joint prediction objective, where the model learns to predict a composite term $\hat{\epsilon}^\theta$ representing the noise and the representation shift together:

$$a^t = \sqrt{\bar{\alpha}_t} a^0 + \underbrace{(1 - \sqrt{\bar{\alpha}_t}) z + \sqrt{1 - \bar{\alpha}_t} \epsilon}_{\hat{\epsilon}^\theta}. \quad (13)$$

Under this scheme, the sampling iteration simplifies as:

$$a^{t-1} = \sqrt{\frac{\bar{\alpha}_{t-1}}{\bar{\alpha}_t}} (a^t - \hat{\epsilon}^\theta) + \frac{\sqrt{1 - \bar{\alpha}_{t-1}}}{\sqrt{1 - \bar{\alpha}_t}} \hat{\epsilon}^\theta \quad (14)$$

In this way, we not only bias the prior distribution, but also introduce extra supervision on each denoising steps to further guide and simplify the denoising process. A complete empirical analysis of these variants can be found in Section 5.3.2, which shows the great policy performance gain of the proposed approach.

5. Experiments

With experiments, we aim to answer these questions:

1. How does the performance of proposed DADP policy compared to existing SOTA methods?
2. Does the proposed Lagged Context Dynamical Prediction contributes to the representation quality?
3. Does the proposed representation utilization further improve the performance of the diffusion policy?

5.1. Experimental Setup

Environments. Previous evaluations of domain adaptation policies have largely focused on existing locomotion settings (Todorov et al., 2012; Ni et al., 2023), where domain randomization typically is restricted to mild variations (e.g., friction or gravity shifts), which tend to have limited impact on the optimal gait. In this work, we expand the locomotion tasks to four environments and further introduce morphological variations. As a result, the gaits across different domains exhibit greater diversity compared to prior works. Please refer to Appendix D.2 for the dataset visualization. Furthermore, to demonstrate the generality and applicability of DADP in environments with complex dynamics, we additionally incorporate a manipulation benchmark, Adroit (Rajeswaran et al., 2017), into our experiments.

Data Generation. For locomotion environments, we follow the data collection pipeline of CORRO (Yuan & Lu, 2022), constructing the task set by sampling different environmental factors in the parametric space. For each task, we use SAC (Haarnoja et al., 2018) to train a task-specific expert for offline data collection, which contains 25 domains. For manipulation tasks in Adroit, we adopt the pre-collected dataset from ODRL (Lyu et al., 2024), which contains 3 domains. Please refer to Appendix B.1 for more details.

Baselines. We consider the following methods as our baselines. Please refer to Appendix B.2 for more details.

- **CORRO** (Yuan & Lu, 2022) proposes a contrastive learning framework for robust task representations under distribution shifts, outperforming prior context-conditioned policy-based methods.
- **Prompt-DT** (Xu et al., 2022) leverages Transformer-based sequence modeling with a prompt formulation to enable few-shot adaptation in offline RL, serving as a strong end-to-end meta-RL baseline.
- **Meta-DT** (Wang et al., 2024b) incorporates an additional learned domain representation as an augmented observation, further improving performance and representing a SOTA baseline in domain adaptation task.

Table 1. Benchmark performance across different environments. The results are from the last checkpoint, which are presented in mean \pm std across 5 random seeds, where the highest mean performance of each variant is bolded, and the second highest is underlined.

Environment	Setting	Expert	CORRO	Prompt-DT	Meta-DT	DADP (Ours)
HalfCheetah	IID	4575	-301 \pm 42	1640 \pm 194	<u>3857</u> \pm 234	4100 \pm 85
	OOD	–	-246 \pm 36	250 \pm 375	3174 \pm 501	<u>3056</u> \pm 113
Walker2d	IID	7101	61 \pm 49	590 \pm 57	<u>1304</u> \pm 586	3991 \pm 24
	OOD	–	66 \pm 69	435 \pm 157	<u>889</u> \pm 579	3015 \pm 207
Ant	IID	3598	-867 \pm 430	700 \pm 189	<u>3045</u> \pm 128	3117 \pm 88
	OOD	–	-962 \pm 553	208 \pm 126	<u>3187</u> \pm 899	3495 \pm 102
Hopper	IID	1555	80 \pm 11	935 \pm 65	<u>1140</u> \pm 156	1643 \pm 37
	OOD	–	61 \pm 21	1148 \pm 150	<u>1208</u> \pm 99	1711 \pm 60
Door	IID	3233	-50 \pm 13	2116 \pm 177	1283 \pm 323	<u>1483</u> \pm 55
	OOD	3261	-58 \pm 2	1080 \pm 209	<u>1294</u> \pm 228	1430 \pm 99
Relocate	IID	-1.92	-12.3 \pm 1.92	-7.44 \pm 0.10	<u>-6.06</u> \pm 0.40	-5.57 \pm 0.24
	OOD	-1.70	-12.0 \pm 0.72	-6.47 \pm 0.36	<u>-5.77</u> \pm 0.42	-5.63 \pm 0.21

Training and Evaluation. Training is conducted in two stages. Firstly, a context encoder is pre-trained on training dataset to extract domain representations from trajectories; secondly, a diffusion policy is trained with the fixed learned context encoder across 5 random seeds.

During evaluation, we test the policies with zero-shot setting, where the contexts are online collected during policy rollout. Compared to the few-shot setting, which assumes access to expert datasets from unseen domains as context, the zero-shot setting more closely reflects practical deployment scenarios (Liu et al., 2025b). We evaluate all the baselines under both In-Distribution (IID) and Out-of-Distribution (OOD) settings. The IID setting measures performance on all the domains present in the training dataset, assessing the policy’s ability to master multiple domains. For the OOD setting, we randomly sample environmental parameters from the factor space to construct 5 new domains, evaluating the policy’s generalizability to unseen domains. For the Adroit benchmark, we instead use the Easy and Hard domains for IID setting, and the Medium domain as the OOD setting. Please refer to Appendix E for more details.

5.2. Experimental Results

As shown in Table 1, across all evaluated environments, DADP consistently achieves strong performance under both IID and OOD settings, outperforming or matching the best-performing baselines in nearly all cases. These results indicate that DADP effectively captures and leverages the domain information to improve performance across in-distribution and out-of-distribution domains. Moreover, across all environments, DADP achieve stable performance with smaller standard deviation value across different seeds, demonstrating its strong stability and practicability.

5.3. Ablation Study

In the ablation study, we aim to examine how each proposed component of our diffusion policy contributes to the overall performance. We focus on the two tasks where DADP achieves the different level of gains over the other baselines in the main results, Walker2d and HalfCheetah. Please refer to Appendix C for additional experiments and analysis.

5.3.1. EFFECT OF Δt ON REPRESENTATION QUALITIES

To evaluate the representation qualities, we apply the learned context encoder to encode the training dataset, obtaining the domain representation set. Specifically, we use the linear probe accuracy (Oord et al., 2018) and reconstruction loss to evaluate the representation qualities. For linear probe accuracy, we train a single-layer softmax linear classifier to predict the one-hot domain index corresponding to each representation; for reconstruction loss, we train a two-layer MLP to predict the exact dynamical parameter vectors. Furthermore, we treat the supervised representation as an upper bound on performance, as it is trained with access to ground-truth labels—specifically in our setting, the environment parameters and the corresponding one-hot domain indices.

As shown in the Table 2, as Δt increases, both metrics consistently improve, eventually comparable to that of supervised representations. This indicates that larger Δt effectively breaks time-local cues, resulting in representations with stronger representative capacity for domain classification and encoding underlying dynamical parameters. Moreover, we can explain the larger performance gain on Walker2d compared with the HalfCheetah, since the former representation quality benefit much more from larger Δt .

We also provide the t-SNE visualizations of the represen-

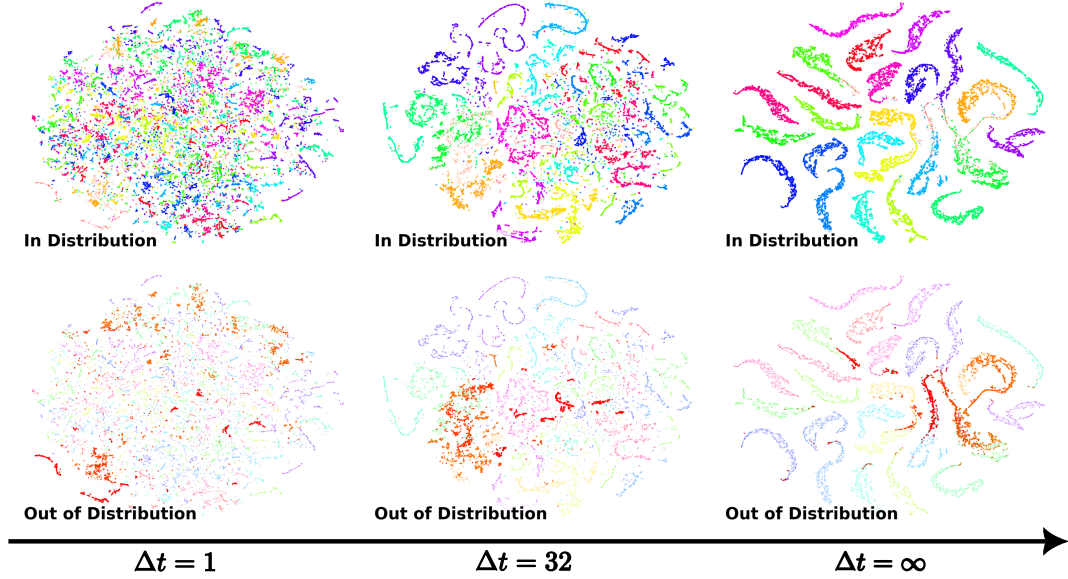


Figure 3. t-SNE visualization of walker representations learned with different Δt .

Table 2. Normalized Representative Metrics of Learned Embeddings with different Δt .

Environment	Metrics	$\Delta t = 1$	$\Delta t = 4$	$\Delta t = 16$	$\Delta t = 32$	$\Delta t = \infty$	Supervised
Walker2d	Linear Probe Accuracy	27.9%	35.7%	48.5%	64.9%	99.3%	99.8%
	Reconstruction Loss	476.1	427.5	312.6	229.0	3.2	1.0
HalfCheetah	Linear Probe Accuracy	68.6%	84.7%	96.7%	98.3%	99.9%	99.9%
	Reconstruction Loss	45.9	19.8	3.4	1.1	0.4	1.0

tations of Walker2d learned with different Δt in figure 3. As Δt increases, the representations from different domains gradually distinctly cluster. Compared some previous methods (Yuan & Lu, 2022; Li et al., 2020) based on contrastive learning, our approach can achieve great embedding qualities from a simple objective without extra data generation.

Furthermore, we validate that the static representation can lead to better policy performance. As shown in Table. 4, conditional policy can benefit from the higher-quality representations, especially in the walker2d, whose representations quality improves more. With the proposed utilization, the performance gain can achieve comparable performance with Supervised baseline whose representation is trained with supervised learning as in Sec. 5.3.1.

We also validate that the performance gain can be consistently achieved across reward-changing environments and different datasets with ablation on Meta-DT. As the results shown in Table 3, by introducing larger Δt to the representation in the Meta-DT, we observe consistent performance gains across all domain adaptive environments and the majority of reward-changing environments, demonstrating the generalizability of the proposed simple yet effective representation learning technique.

Table 3. Meta-DT performance with different Δt .

Environment	$\Delta t = 1$	$\Delta t = 32$
Point-Robot	-10.7	-11.6
Ant-Dir	368.9	391.7
Cheetah-Dir	542.4	554.2
Cheetah-Vel	-100.1	-98.7
Hopper-Param	342.0	363.6
Walker-Param	397.4	399.8

5.3.2. EFFECT OF REPRESENTATION UTILIZATION

In this section, we investigate how different representation utilization affect the resulting policy performance. Specifically, we mainly focus on the following utilizations:

1. **Null.:** We remove the representation in policy input and generation, serving as an end-to-end baseline.
2. **Cond.:** We utilize the representation as the extra input to the policy for conditional generation.
3. **w/o Predict:** We utilize the representation to bias the prior distribution to a mixed gaussian.
4. **w/ Predict:** Upon w/o Predict, we further utilize the representation as part of policy prediction target.

Table 4. Ablation Results on Representation Utilization.

Variants	Options		Walker2d			HalfCheetah		
	Representation	Utilization	IID	OOD	Mastery	IID	OOD	Mastery
End-to-End Diffusion	Null.	Null.	3722	2852	40%	3509	2496	80%
Conditional Policy	$\Delta t = 1$	Cond.	2093	1617	0%	3740	2594	80%
Better Representation	$\Delta t = \infty$	Cond.	3394	1813	28%	3603	2744	76%
Mixed DDIM	$\Delta t = \infty$	w/o Predict	3356	1908	36%	3533	3012	84%
DADP (Ours)	$\Delta t = \infty$	w/ Predict	3991	3015	44%	4100	3055	96%
Expert	Null.	Null.	7101	-	100%	4575	-	100%
Supervised	Supervised	w/ Predict	4014	2540	44%	3846	3152	88%

As shown in Table 4, DADP achieve superior performance across all the variants. This indicates that our proposed utilization strategy maximizes the effectiveness of the learned high-quality representations.

To validate the source of performance gain, we introduce a new metric, *mastery*, which is ratio of IID domains that policy achieve 60% of the expert policy performance. Across all the variants, DADP achieves the highest mastery, showing its strong capability to master diverse domains and locate the target manifold of the corresponding domain, resulting better mastery across the domains. In real-world application, higher mastery implies that a single policy can adapt to a broader range of embodiments and diverse environments. Please refer to Appendix D.2 for visualization results.

To visualize if the representation-prediction utilization can enable effective denoising process, we first rollout the corresponding variants in a specific domain. Next, we split the trajectories into contexts, apply the learned context encoder and visualize the representations of the resulting trajectories. As shown in Figure 4, compared with Mixed DDIM and Conditional Policy, DADP representation accurately locate the running policy to the target domain thus better leverage the in-distribution capability for better control performance.

Another interesting observation is, despite its simplicity, End-to-End Diffusion outperforms many variants. This suggests that diffusion-based policies constitute a particularly well-suited policy architecture for domain adaptation problems, and remain underexplored in this context.

6. Conclusion

We propose DADP, a diffusion policy achieves robust domain adaptation through unsupervised disentanglement and domain-aware diffusion injection. To obtain high-quality domain representations unsupervisedly, we propose Lagged Context Dynamical Prediction to remove the time-varying

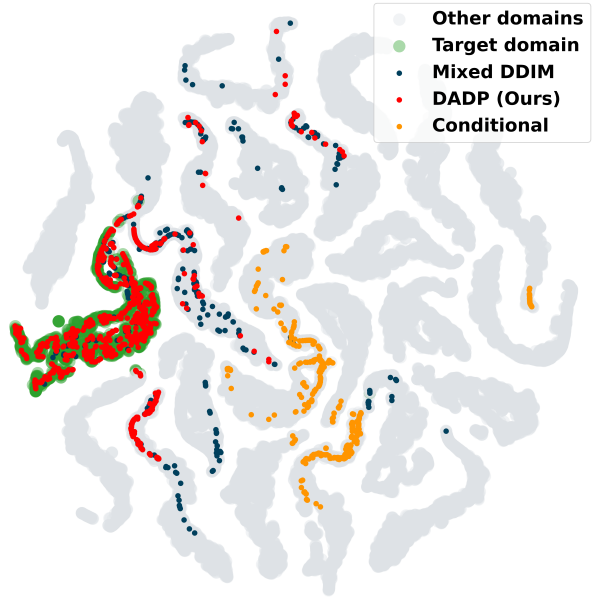


Figure 4. Walker Online Adaptation Representation Visualizations

information presents in the context. With the learned representations, we bias the prior distribution and reformulate the diffusion target, achieving SOTA performance and generalizability across diverse challenging benchmarks with verifiable analysis and visualization.

Limitations. In this work, we focus on stationary (time-invariant) dynamics and therefore distangle static information from the time-varying information in the context. Nonetheless, time-varying signals can be crucial in non-stationary environments, where they may reflect evolving dynamics that a policy must track for effective control. In future work, we plan to explore how to jointly disentangle and retain the time-varying information, and extend DADP to non-stationary dynamical environments settings.

References

Barreto, A., Dabney, W., Munos, R., Hunt, J. J., Schaul, T., van Hasselt, H. P., and Silver, D. Successor features for transfer in reinforcement learning. *Advances in neural information processing systems*, 30, 2017.

Chen, L., Lu, K., Rajeswaran, A., Lee, K., Grover, A., Laskin, M., Abbeel, P., Srinivas, A., and Mordatch, I. Decision transformer: Reinforcement learning via sequence modeling. *Advances in neural information processing systems*, 34:15084–15097, 2021.

Chi, C., Xu, Z., Feng, S., Cousineau, E., Du, Y., Burchfiel, B., Tedrake, R., and Song, S. Diffusion policy: Visuomotor policy learning via action diffusion. *The International Journal of Robotics Research*, 44(10-11): 1684–1704, 2025.

Dai, Z., Yang, Z., Yang, Y., Carbonell, J. G., Le, Q., and Salakhutdinov, R. Transformer-xl: Attentive language models beyond a fixed-length context. In *Proceedings of the 57th annual meeting of the association for computational linguistics*, pp. 2978–2988, 2019.

Duan, Y., Schulman, J., Chen, X., Bartlett, P. L., Sutskever, I., and Abbeel, P. RI 2: Fast reinforcement learning via slow reinforcement learning. *arXiv preprint arXiv:1611.02779*, 2016.

Evans, B., Thankaraj, A., and Pinto, L. Context is everything: Implicit identification for dynamics adaptation. In *2022 International Conference on Robotics and Automation (ICRA)*, pp. 2642–2648. IEEE, 2022.

Haarnoja, T., Zhou, A., Abbeel, P., and Levine, S. Soft actor-critic: Off-policy maximum entropy deep reinforcement learning with a stochastic actor. In *International conference on machine learning*, pp. 1861–1870. Pmlr, 2018.

He, T., Gao, J., Xiao, W., Zhang, Y., Wang, Z., Wang, J., Luo, Z., He, G., Sobanbab, N., Pan, C., et al. Asap: Aligning simulation and real-world physics for learning agile humanoid whole-body skills. *arXiv preprint arXiv:2502.01143*, 2025.

Ho, J., Jain, A., and Abbeel, P. Denoising diffusion probabilistic models. *Advances in neural information processing systems*, 33:6840–6851, 2020.

Hu, Z., Xu, T., Xiao, X., and Wang, X. Carol: Context-aware adaptation for robot learning. *arXiv preprint arXiv:2506.07006*, 2025.

Huang, S., Hu, J., Yang, Z., Yang, L., Luo, T., Chen, H., Sun, L., and Yang, B. Decision mamba: Reinforcement learning via hybrid selective sequence modeling. *Advances in Neural Information Processing Systems*, 37: 72688–72709, 2024.

Jia, N., Zhu, T., Liu, H., and Zheng, Z. Structured diffusion models with mixture of gaussians as prior distribution, 2024. URL <https://arxiv.org/abs/2410.19149>.

Kumar, A., Fu, Z., Pathak, D., and Malik, J. Rma: Rapid motor adaptation for legged robots. *arXiv preprint arXiv:2107.04034*, 2021.

Kumar, A., Li, Z., Zeng, J., Pathak, D., Sreenath, K., and Malik, J. Adapting rapid motor adaptation for bipedal robots. In *2022 IEEE/RSJ International Conference on Intelligent Robots and Systems (IROS)*, pp. 1161–1168. IEEE, 2022.

Laskin, M., Wang, L., Oh, J., Parisotto, E., Spencer, S., Steigerwald, R., Strouse, D., Hansen, S., Filos, A., Brooks, E., et al. In-context reinforcement learning with algorithm distillation. *arXiv preprint arXiv:2210.14215*, 2022.

Lee, K., Seo, Y., Lee, S., Lee, H., and Shin, J. Context-aware dynamics model for generalization in model-based reinforcement learning. In *International Conference on Machine Learning*, pp. 5757–5766. PMLR, 2020.

Li, L., Yang, R., and Luo, D. Focal: Efficient fully-offline meta-reinforcement learning via distance metric learning and behavior regularization. *arXiv preprint arXiv:2010.01112*, 2020.

Liu, J., Liu, F., Hao, J., Wang, B., Li, H., Chen, C., and Wang, Z. Scalable in-context q-learning. *arXiv preprint arXiv:2506.01299*, 2025a.

Liu, M., Pathak, D., and Agarwal, A. Locoformer: Generalist locomotion via long-context adaptation. In *Conference on Robot Learning*, pp. 532–546. PMLR, 2025b.

Lu, H., Han, D., Shen, Y., and Li, D. What makes a good diffusion planner for decision making? *arXiv preprint arXiv:2503.00535*, 2025.

Lyu, J., Xu, K., Xu, J., Yan, M., Yang, J., Zhang, Z., Bai, C., Lu, Z., and Li, X. Odrl: A benchmark for off-dynamics reinforcement learning. In *The Thirty-eight Conference on Neural Information Processing Systems Datasets and Benchmarks Track*, 2024. URL <https://openreview.net/forum?id=ap4x1kArGy>.

Lyu, J., Li, Z., Shi, X., Xu, C., Wang, Y., and Wang, H. Dywa: Dynamics-adaptive world action model for generalizable non-prehensile manipulation. *arXiv preprint arXiv:2503.16806*, 2025.

Ni, F., Hao, J., Mu, Y., Yuan, Y., Zheng, Y., Wang, B., and Liang, Z. Metadiffuser: Diffusion model as conditional planner for offline meta-rl. In *International Conference on Machine Learning*, pp. 26087–26105. PMLR, 2023.

Oord, A. v. d., Li, Y., and Vinyals, O. Representation learning with contrastive predictive coding. *arXiv preprint arXiv:1807.03748*, 2018.

Ota, T. Decision mamba: Reinforcement learning via sequence modeling with selective state spaces. *arXiv preprint arXiv:2403.19925*, 2024.

Rajeswaran, A., Kumar, V., Gupta, A., Vezzani, G., Schulman, J., Todorov, E., and Levine, S. Learning complex dexterous manipulation with deep reinforcement learning and demonstrations. *arXiv preprint arXiv:1709.10087*, 2017.

Song, J., Meng, C., and Ermon, S. Denoising diffusion implicit models, 2022. URL <https://arxiv.org/abs/2010.02502>.

Su, Z., Zhang, B., Rahamanian, N., Gao, Y., Liao, Q., Regan, C., Sreenath, K., and Sastry, S. S. Hitter: A humanoid table tennis robot via hierarchical planning and learning. *arXiv preprint arXiv:2508.21043*, 2025.

Todorov, E., Erez, T., and Tassa, Y. Mujoco: A physics engine for model-based control. In *2012 IEEE/RSJ international conference on intelligent robots and systems*, pp. 5026–5033. IEEE, 2012.

Wang, M., Bing, Z., Yao, X., Wang, S., Kai, H., Su, H., Yang, C., and Knoll, A. Meta-reinforcement learning based on self-supervised task representation learning. In *Proceedings of the AAAI Conference on Artificial Intelligence*, volume 37, pp. 10157–10165, 2023.

Wang, P., Li, C., Weaver, C., Kawamoto, K., Tomizuka, M., Tang, C., and Zhan, W. Residual-mppi: Online policy customization for continuous control. *arXiv preprint arXiv:2407.00898*, 2024a.

Wang, Z., Zhang, L., Wu, W., Zhu, Y., Zhao, D., and Chen, C. Meta-dt: Offline meta-rl as conditional sequence modeling with world model disentanglement. *Advances in Neural Information Processing Systems*, 37:44845–44870, 2024b.

Wen, X., Bai, C., Xu, K., Yu, X., Zhang, Y., Li, X., and Wang, Z. Contrastive representation for data filtering in cross-domain offline reinforcement learning. *arXiv preprint arXiv:2405.06192*, 2024.

Xu, M., Shen, Y., Zhang, S., Lu, Y., Zhao, D., Tenenbaum, J., and Gan, C. Prompting decision transformer for few-shot policy generalization. In *international conference on machine learning*, pp. 24631–24645. PMLR, 2022.

Yuan, H. and Lu, Z. Robust task representations for offline meta-reinforcement learning via contrastive learning. In *International Conference on Machine Learning*, pp. 25747–25759. PMLR, 2022.

Zhang, X., Liu, S., Huang, P., Han, W. J., Lyu, Y., Xu, M., and Zhao, D. Dynamics as prompts: In-context learning for sim-to-real system identifications. *IEEE Robotics and Automation Letters*, 2025.

A. Toy case of Δt Design

The toy case can be illustrated with Figure 5. We consider a toy example of a ball vertical projectile motion under gravity without air resistance, whose time-step length t_0 is known. At each time step, the state of the ball is represented solely by its vertical position $s_t = y_t$, which constitutes an incomplete state representation without the vertical speed v_t^y . Our goal is to infer the unique scalar environmental factor of this system—the gravitational acceleration g —by predicting the next state:

$$y_{t+1} = y_t + v_t^y t_0 + \frac{1}{2} g t_0^2 \quad (15)$$

Consider the prediction with the most recent context with $\Delta t = 1$, $\tau_{\Delta t=1} = (y_{t-3}, y_{t-2}, y_{t-1})$, which is encoded as $z_{\Delta t=1} = E_\phi(\tau_{\Delta t=1})$. Note that for continuous states of length $L = 3$, there are always two types of information that can be extracted from the sequence (y_{T-2}, y_{T-1}, y_T) .

- **Static gravity** $g = \frac{1}{t_0^2} (y_T + y_{T-2} - 2y_{T-1})$
- **Varying speed** $v_T^y = \frac{1}{2t_0} (4y_{T-1} - 3y_{T-2} - y_T)$

Due to the time-local cues, the extracted velocity from the context can assist the prediction to achieve lower prediction loss by extend itself to the current step.

$$v_t^y = v_{t-1}^y + gt_0 = v_T^y + gt_0 \quad (16)$$

We assume that the neural network can eventually achieve zero loss on this prediction; under this assumption, the learned representation must encode both types of information:

$$z_{\Delta t=1} = \arg \min_{z=(g_z, v_z)} \mathbb{E} \|y_{t+1} - \hat{y}_{t+1}\|^2 = \arg \min_{z=(g_z, v_z)} \mathbb{E} \|g - g_z\|^2 + \|v_t^y - v_z\|^2 = (g, v_{t-1}^y + gt_0) \quad (17)$$

However, this makes the representation a mixture of varying information and static domain representation, while only the latter is desired for representation learning. To remove the time-varying component, one can reduce the influence of time-local cues by simply increasing the Δt , namely the distance between the context and the current step.

Now consider the context from another episode in the same domain $\tau_{\Delta t=\infty} = (y_{t-3}, y_{t-2}, y_{t-1})$. In this case, the varying speed can not be extended to the current step. To predict next state with lowest loss, the encoder would be enforced to learn the static information: gravitational acceleration g and the averaged velocity $\bar{v}^y = \mathbb{E}_{\mathcal{D}} [v_t^y]$:

$$z_{\Delta t=\infty} = \arg \min_{z=(g_z, v_z)} \mathbb{E} \|y_{t+1} - \hat{y}_{t+1}\|^2 = \arg \min_{z=(g_z, v_z)} \mathbb{E} \|g - g_z\|^2 + \|v_t^y - v_z\|^2 = (g, \bar{v}^y) \quad (18)$$

In this case, we recover a static estimate of the gravitational acceleration. Meanwhile, the additionally learned average velocity term serves as complementary static information that characterizes the overall distribution, enabling the representation to remain stable within each domain while also capturing salient behavioral patterns.

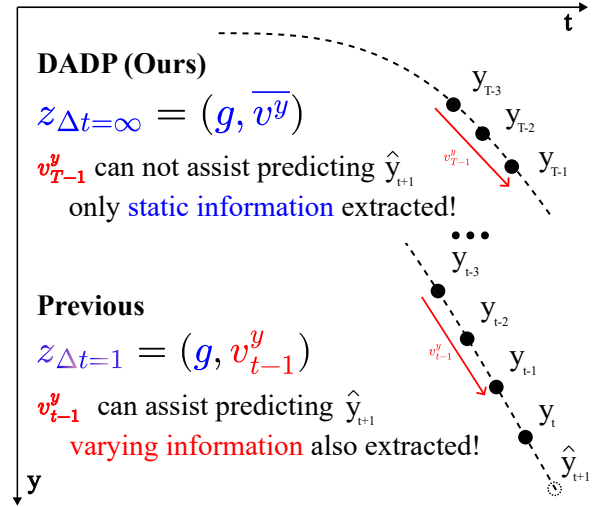


Figure 5. Intuition of the Δt design: since the varying velocity inferred from another episode in the same domain can not assist the prediction, only static gravity will be extracted in the representation.

B. Implementation Details

B.1. Expert Dataset

Dataset Generation. We generated datasets across four MuJoCo environments: Ant, HalfCheetah, Walker2d, and Hopper. For each environment, we varied specific physical parameters to create diverse dynamics. For Ant, HalfCheetah, and Hopper, the datasets comprise 25 distinct sets of dynamics parameters, with each set containing 100 episodes. Due to the higher complexity of the Walker2d environment, we generated 25 distinct dynamics parameters with 300 episodes per set to ensure sufficient coverage. The maximum episode length is set to 1,000 transitions. Due to its inherent instability of Hopper expert data generation, we limit its transitions to 500 and do not introduce morphological variations. To generate the data, we trained a Soft Actor-Critic (SAC) policy for each parameter setting and collected rollouts from the resulting policies.

For the Adroit manipulation domain, we utilized datasets from (Lyu et al., 2024), specifically selecting the *relocate-shrink-finger* and *door-shrink-finger* tasks. Following the benchmark protocols, we used the "Easy" and "Hard" variants for training. Refer to (Lyu et al., 2024) for the specific configurations of these tasks.

Table 5. Dynamics parameter ranges for the MuJoCo environments.

Environment	Parameter	Range
Ant	Leg Length (4 legs)	[0.465, 1.612]
Hopper	Joint Damping (3 joints)	[0.75, 1.19]
	Friction	[0.75, 1.19]
HalfCheetah	Back Leg Mass	[2.99, 6.69]
	Torso Length	[0.336, 0.951]
	Head Length	[0.084, 0.238]
	Front Leg Lengths	[0.075, 0.400]
Walker2d	Friction	[1.32, 2.28]
	Torso / Foot Length	[0.30, 0.67]
	Thigh / Leg Length	[0.27, 0.51]
	Mass (Left Thigh/Leg/Foot)	[2.99, 6.69]

B.2. Baselines

We benchmark our method against four baselines representing distinct training paradigms, including an offline RL-based approach, two Decision Transformer (DT)-based approaches, and one diffusion-based approach. For reproducibility, we utilize the official implementations for all baselines, with specific adaptations for our setting as detailed below:

CORRO (Yuan & Lu, 2022). We employ the official implementation of this robust offline meta-RL method. It utilizes contrastive learning to acquire robust task representations, generating a latent representation from the task context. The offline RL policy is then conditioned on this representation to handle distribution shifts effectively.

Prompt-DT (Xu et al., 2022). Building on the official Decision Transformer implementation, this method utilizes trajectory segments as prompts to encode task information. While the standard inference pipeline samples prompts from an expert dataset, we modify this process to ensure a fair comparison under our zero-shot setting. Specifically, we construct the prompt using the agent's recent interaction history directly gathered from the environment.

Meta-DT (Wang et al., 2024b). We utilize the official Meta-DT codebase, which trains an encoder to compress trajectory segments into latent representations. These representations are processed by a world model (comprising a dynamics decoder and reward decoder). A Decision Transformer then conditions on this representation to predict future actions. In our experiments, as we focus exclusively on dynamics shifts, the reward decoder component is omitted.

End-to-End Diffusion (Lu et al., 2025). We adopt the modular architecture from the official implementation of DV (Lu et al., 2025), which decomposes the diffusion policy into three distinct components: a planner, reward guidance, and an optional inverse dynamics policy. In our deployment, we utilize a Diffusion Transformer (DiT) as the backbone for the planner. To inject dynamics information, we condition the planner on the history trajectory and utilize the diffusion model to inpaint the future trajectory. Consistent with DADP, we exclude the reward guidance module.

B.3. The details of DADP

Context Encoder Architecture: The context encoder is implemented with a Transformer encoder with adaptive pooling at the output layer. Specifically, Two separate MLPs (state/ action encoder) map raw state and actions to the same dimension, and interleave the state tokens and action tokens to form a token sequence. Next, add learnable positional representations and apply dropout, and feed the position-augmented tokens into a Transformer encoder to produce output. Finally, aggregate the sequence using a learnable-query multi-head attention pooling to get a single vector as the representation.

Diffusion Policy Architecture: The diffusion policy in DADP is adapted from the official implementation of DV. We modify the forward and denoising processes according to the formulations in (9)–(14). All other components, including model hyperparameters and network architecture, remain identical to the original DV implementation.

The corresponding hyperparameters are shown in Table 6.

Table 6. Context Encoder Hyperparameters and Experimental Settings

Hyperparameter	Value
<i>Context Encoder Architecture</i>	
Model Dimension	256
MLP Hidden Dimension	256
Feedforward Hidden Dimension	1024
Hidden Layer	4
Adaptive Pooling Heads	8
Adaptive Pooling Dropout	0.1
Attention Heads	8
History Length (H)	16
Task Representation Dim.	$\dim(s) + \dim(a)$
<i>Context Encoder Training</i>	
Batch Size	128
β_{forward}	1.0
β_{inverse}	1.0
Training Ratio	0.8
Learning Rate	3e-4
Epochs	10
<i>Policy Architecture</i>	
Hidden Dimension	256
Planner Depth	6
Attention Heads	8
History Length (H)	16
Prediction Horizon	4
Noise Schedule	Cosine
<i>Policy Training</i>	
Batch Size	256
Learning Rate	3e-4
MuJoCo Iterations	1e6 (Walker), 4e5 (Ant, Hopper), 1e5 (HalfCheetah)
Adroit Iterations	5e5 (Relocation), 1e5 (Door)
<i>Inference & Evaluation</i>	
Inference Steps	5
Guidance Scale	0.1 (Ant: 0.05)
Max Env Steps	1000 (MuJoCo), 200 (Adroit)
Eval. Episodes	50 (MuJoCo), 200 (Adroit)

C. Additional Experiments

C.1. Effect of different guidance scale

In this section, we conduct an ablation study over a range of values for the introduced guidance scale. As shown in Table 7, the results indicate that our method is not highly sensitive to this coefficient, with performance degrading sharply only when the guidance scale becomes excessively large. This demonstrates that our approach can achieve excellent performance without requiring extensive hyperparameter tuning.

Table 7. Ablation Results under Different Guidance Scales.

Environment	Setting	0	0.01	0.05	0.1	0.5	1	5
Walker2d	IID	3722	4026	4231	3957	3968	3615	2759
	OOD	2852	2721	2837	2681	2934	<u>2891</u>	1854
HalfCheetah	IID	3509	3920	3808	4079	4114	<u>4093</u>	404.5
	OOD	2496	2931	2604	<u>3021</u>	2934	3162	39.5

C.2. Context Source

In DADP, since the representation represents static domain information, its context source is not restricted to online-collected recent history. In this section, we further consider several practical deployment settings to substantiate the properties of the learned representations and the general applicability of DADP. We continue to assume that, in an unknown domain, no ground-truth policy rollouts are available, as this represents the most realistic scenario when deploying a policy to a new domain. Specifically, we consider the following three variants of context source:

- **Cold Start:** DADP adopted approach, whose context is online collected recent history. When the online recent history length is insufficient, padding states and actions are used to complete the context window.
- **Persistent Context:** By executing the Cold Start policy, we have the in-domain policy rollouts as context source. We randomly sample a clip in the policy rollouts as the persistent context used during online inference.
- **Warm Start:** Following the Persistent Prompt, we replace the context source from policy rollouts to online recent history when length is sufficient. The context from policy rollouts is only used as warm start prompt.

Table 8. Ablation Results on Context Source. The normalized metric is the averaged performance normalized with the Expert IID.

Variants	Walker2d		HalfCheetah		Hopper		Ant		Normalized	
	IID	OOD	IID	OOD	IID	OOD	IID	OOD	IID	OOD
Cold Start	3985	2765	4079	3045	1692	1809	3069	3414	0.851	0.797
Persistent Context	3988	2938	4080	2902	1679	1828	3206	3552	0.858	0.809
Warm Start	4117	2833	4070	2846	1688	1662	3221	3670	0.865	0.783

We evaluate the different variants with the same checkpoint across the MuJoCo environments. As shown in Table 8, different variants achieve comparable performance, further validating the static nature of the learned representations and the resulting flexibility in the choice of context sources. Moreover, this property enables the use of pre-collected rollouts obtained by executing the policy in the environment to mitigate the cold-start phase with incomplete context, thereby improving stability and performance once the context is fully populated.

D. Visualization

D.1. Representation Visualization

We also provide the t-SNE visualizations of the representations of HalfCheetah learned with different Δt in figure 6. As Δt increases, the representations from different domains also become gradually distinctly clustered.

We observe from the quantitative results that, in Walker2d, increasing Δt yields a substantially larger improvement in representation quality compared to HalfCheetah. This trend is also reflected in the visualization: when $\Delta t = 1$, different domains already exhibit partial clustering behavior, and for some domains, increasing Δt leads to improved cluster separation. As $\Delta t \rightarrow \infty$, the resulting representations achieve high quality comparable to those observed in the Walker2d setting.

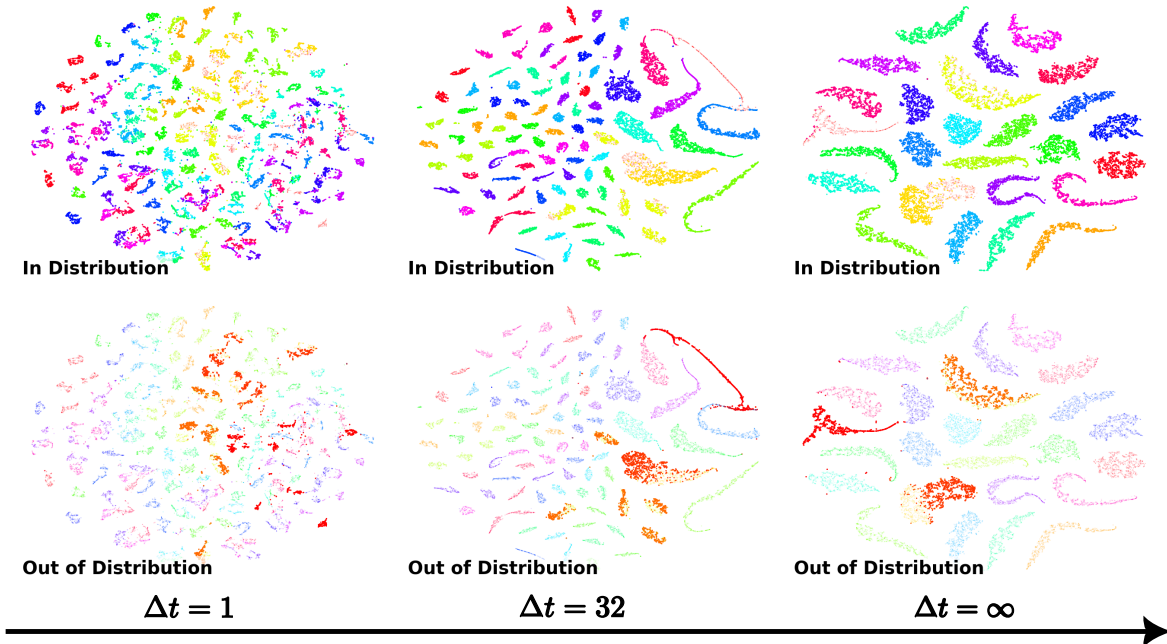


Figure 6. t-SNE visualization of half cheetah representations learned with different Δt .

D.2. Domain-specific Action Modalities

In this section, we provide visualizations of different domain-specific gaits presented in different tasks in Figure 7, 8, 9, 10.

As mentioned in Appendix B.1, we do not introduce morphological variations in the Hopper environment for better and more stable expert data generation. As shown in Figure 7, without morphological variations, the gaits across different domains are similar, resulting in reduced data diversity. This aligns with our analysis on previous benchmarks.

As shown in Figure 8, 9, 10, it is clear that by introducing morphological variations during the data generation phase, the gaits and action modalities across different domains become substantially more diverse, thereby constructing a more challenging domain adaptation benchmark. Despite that, our proposed method is able to achieve state-of-the-art performance in environments with substantial dynamical gaps, demonstrating its broader applicability compared to prior approaches.

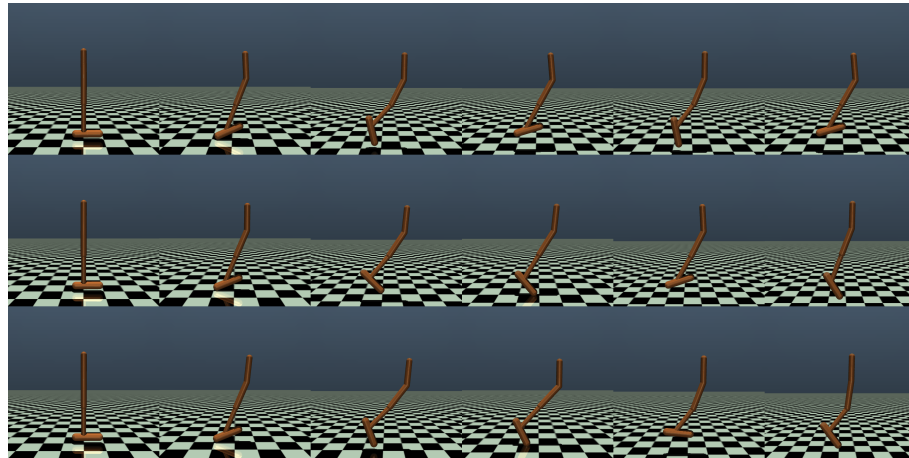


Figure 7. Different Domain-specific Gaits in Hopper. Without morphological variations, the gaits are similar across different domains.

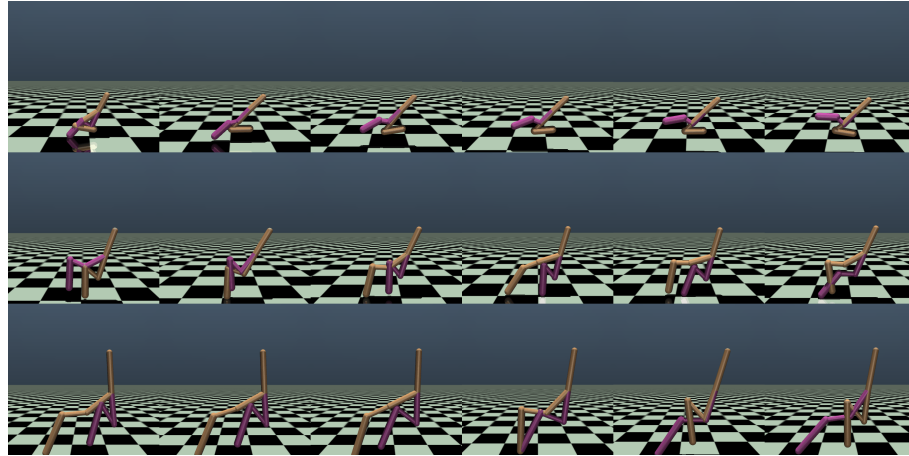


Figure 8. Different Domain-specific Gaits in Walker

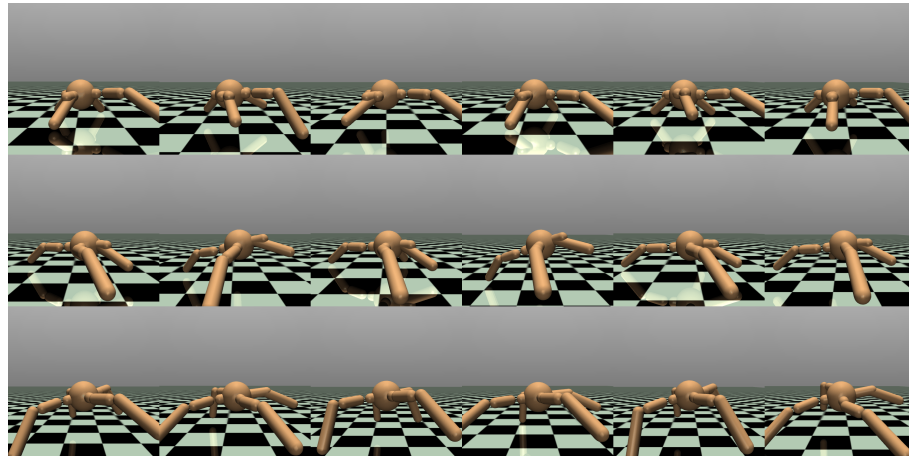


Figure 9. Different Domain-specific Gaits in Ant

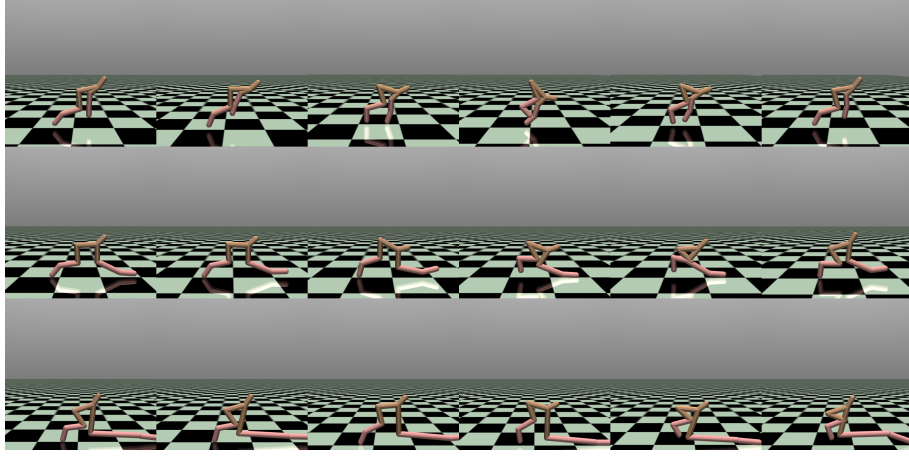


Figure 10. Different Domain-specific Gaits in HalfCheetah

D.3. Mastery Level

In this section, we provide visualizations of the mastery. Here, mastery refers to a policy’s ability to successfully handle multiple domains, reflecting whether a single policy can robustly control different domains or embodiments, which directly impacts its practical effectiveness. As shown in Figure 11, in Walker2d, a policy with high mastery level is able to run forward rapidly and stably for an extended duration (top row). In contrast, policies that achieve non-zero returns but fail to reach mastery exhibit suboptimal gaits (middle row), or even collapse and fall (bottom row). A similar pattern can be observed in HalfCheetah, as illustrated in Figure 12.

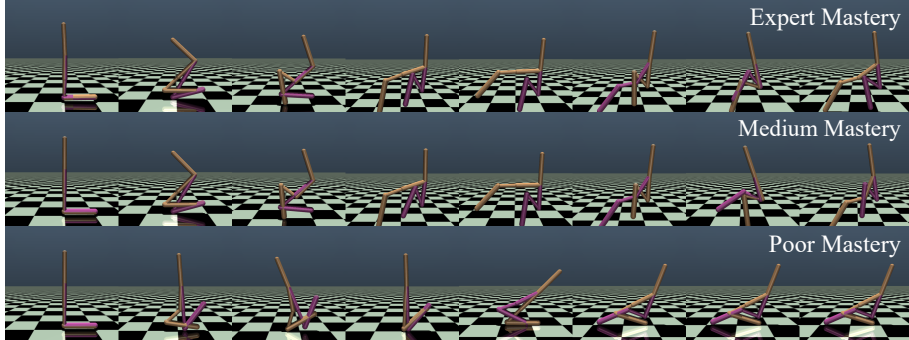


Figure 11. Mastery Level Visualization in Walker2d Environments

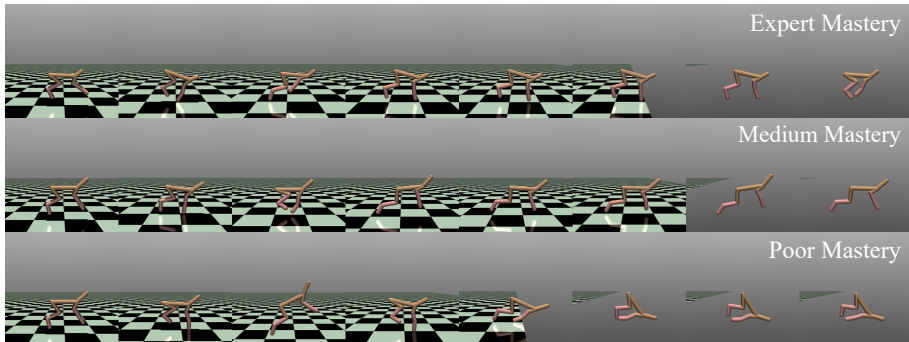


Figure 12. Mastery Level Visualization in HalfCheetah Environments

E. Pesudocodes

In this section, we present the pesudocodes of the proposed DADP pipeline.

Algorithm 1 Domain Adaptive Diffusion Policy (DADP)

Domain Representation Learning

Input: Offline datasets \mathcal{D} , context encoder E_ϕ , forward dynamics model f_θ , inverse dynamics model f_ψ

for each epoch **do**

 Rebuild random domain-based paired index $j = f(i)$

while epoch not finished \mathcal{D} **do**

 Sample paired data $\tau^i, s_{t_j}^j, a_{t_j}^j, s_{t_j+1}^j$

 Get context representation $z^i = E_\phi(\tau^i)$

 Get dynamical prediction $\hat{s}_{t_j+1}^j = f_\theta(s_{t_j}^j, a_{t_j}^j, z^i), \hat{a}_{t_j}^j = f_\psi(s_{t_j}^j, s_{t_j+1}^j, z^i)$ *// Cross-Prediction*

 Update ϕ, θ, ψ with loss: $\mathcal{L}(\phi, \theta, \psi) := \beta_{\text{forward}} \|\hat{s}_{t_j+1}^j - s_{t_j+1}^j\|^2 + \beta_{\text{inverse}} \|\hat{a}_{t_j}^j - a_{t_j}^j\|^2$

end while

end for

DADP Training

Input: Dataset \mathcal{D} , Denoising Schedule $\alpha_{1:K}, \sigma_{1:K}$, Guidance Scale λ , Denoising Policy ϵ_ξ

while not converged **do**

1. Data Sampling & Preparation

 Sample batch $(\tau, z_{\text{pre}}) \sim \mathcal{D}$ *// Sample trajectories and precomputed representations*
 Set $x_0 = \tau$ and M s.t. $M_{t < H} = 1$ and $M_{H, \text{obs}} = 1$ *// Initialize clean data and history mask*

2. Forward Process

 Sample time $k \sim \text{Uniform}(0, 1)$, noise $\epsilon \sim \mathcal{N}(0, I)$
 $x_k^{\text{raw}} = \alpha_k(x_0 - \lambda z) + \lambda z + \sigma_k \epsilon$ *// Mixed gaussian prior*
 $x_k = (1 - M) \odot x_k^{\text{raw}} + M \odot x_0$ *// Keep History for inpainting*

3. Reverse Process

$\hat{\epsilon} = \epsilon_\xi(x_k, k)$
 Update with Loss: $\mathcal{L}_\xi = \|(\sigma_k \epsilon + (1 - \alpha_k) \lambda z - \hat{\epsilon}) \odot (1 - M)\|^2$

end while

DADP Evaluation

Input: History Context h_{ctx} , Sampling Steps S , Guidance Scale λ , Context Encoder E_ϕ , Denoising Policy ϵ_ξ

Output: Action a_H

 Compute Representation $z = E_\phi(h_{\text{ctx}})$
 Sample $\epsilon \sim \mathcal{N}(0, I)$,
 Set M s.t. $M_{t < H} = 1$ and $M_{H, \text{obs}} = 1$ *// Initialize with mixed noise and masking*
 $x_K^{\text{raw}} = \lambda z + \epsilon$ *// Sample from mixed gaussian*
 $x_K = (1 - M) \odot x_K^{\text{raw}} + M \odot h_{\text{ctx}}$ *// Keep History for inpainting*

2. Denoising Loop

for $i = S, \dots, 1$ **do**

 Map i to diffusion times k and $k - 1$
 $\hat{\epsilon} = \epsilon_\xi(x_k, k)$ *// Noise Prediction*
 $x_{k-1}^{\text{raw}} = \frac{\alpha_{k-1}}{\alpha_k} (x_k - \hat{\epsilon}) + \frac{\sigma_{k-1}}{\sigma_k} \hat{\epsilon}$ *// Denoise Step*
 $x_{k-1} = (1 - M) \odot x_{k-1}^{\text{raw}} + M \odot h_{\text{ctx}}$ *// Keep History for inpainting*

end for

3. Execution

 Extract action: $a_H = x_0[H, \text{actions}]$
return a_H